

Anomalous second ferromagnetic phase transition as a signature of spinodal decomposition in Fe-doped GeTe diluted magnetic semiconductor

F. Tong, J. H. Hao, Z. P. Chen, G. Y. Gao, H. Tong et al.

Citation: *Appl. Phys. Lett.* **99**, 202508 (2011); doi: 10.1063/1.3663550

View online: <http://dx.doi.org/10.1063/1.3663550>

View Table of Contents: <http://apl.aip.org/resource/1/APPLAB/v99/i20>

Published by the [American Institute of Physics](http://www.aip.org).

Related Articles

Magnetic transitions in erbium at high pressures

J. Appl. Phys. **111**, 07E104 (2012)

Synthesis, microstructure and magnetic properties of low Nd content Fe₉₀Nd₅B_{3.5}M_{1.5} (M = Hf, Ti and Ta) alloys

J. Appl. Phys. **111**, 07B501 (2012)

Asymmetric switching behavior in perpendicularly magnetized spin-valve nanopillars due to the polarizer dipole field

Appl. Phys. Lett. **100**, 062404 (2012)

Electron resonance and magnetic response of low-doped La_{0.88}Ca_{0.12}MnO₃ and La_{0.9}Sr_{0.1}MnO₃ manganite single crystals

J. Appl. Phys. **111**, 07D702 (2012)

Entropy change linked to the magnetic field induced Morin transition in Hematite nanoparticles

Appl. Phys. Lett. **100**, 063102 (2012)

Additional information on *Appl. Phys. Lett.*

Journal Homepage: <http://apl.aip.org/>

Journal Information: http://apl.aip.org/about/about_the_journal

Top downloads: http://apl.aip.org/features/most_downloaded

Information for Authors: <http://apl.aip.org/authors>

ADVERTISEMENT



Anomalous second ferromagnetic phase transition as a signature of spinodal decomposition in Fe-doped GeTe diluted magnetic semiconductor

F. Tong,^{1,2,3} J. H. Hao,^{2,a)} Z. P. Chen,³ G. Y. Gao,² H. Tong,^{1,3} and X. S. Miao^{1,3,4,a)}¹Wuhan National Laboratory for Optoelectronics, Wuhan 430074, China²Department of Applied Physics, The Hong Kong Polytechnic University, Hong Kong, China³Department of Electronic Science and Technology, Huazhong University of Science and Technology, Wuhan 430074, China⁴Wuhan National High Magnetic Field Center, Wuhan 430074, China

(Received 5 October 2011; accepted 30 October 2011; published online 18 November 2011)

Structural and magnetic properties of diluted magnetic semiconductor $\text{Ge}_{1-x}\text{Fe}_x\text{Te}$ thin films are investigated. The conventional structure analysis shows c -axis orientation with columnar growth of the films and no indication of Fe clusters or second phase. Magnetic measurements combined with theory models reveal that two ferromagnetic phase transitions occur. We consider that the second ferromagnetic phase transition in high Fe content thin film is from a ferromagnetic phase with long range exchange interaction to a superparamagnetic phase with dipole interaction between Fe clusters, which can be viewed as a signature of spinodal decomposition in $\text{Ge}_{1-x}\text{Fe}_x\text{Te}$ material.

© 2011 American Institute of Physics. [doi:10.1063/1.3663550]

Spin manipulation has attracted much attention in last decades. It is mainly based on the diluted magnetic semiconductors (DMSs) which are synthesized by substituting magnetic or appropriate rare earth ions onto lattice sites of the host semiconductors.¹ Extensive studies have been done to explore suitable DMSs for spintronic devices. But all the efforts face the question: whether the ferromagnetism in DMSs comes from inherent exchange interaction or magnetic clusters caused by spinodal decomposition.² For example, the III-V DMS InMnAs has been applied to fabricate the spin injector. However, the Mn rich nano-clusters is observable.³ A promising II-VI DMS Co-ZnO has been found to have high Curie temperature (T_c). But whether the magnetic property is inherent or not is suspectable.⁴ Spinodal decomposition is known to cause the aggregation of magnetic ions in the host semiconductor but does not involve the precipitation of another phase and therefore is hard to detect experimentally.² This makes the research of DMSs into a contradictory situation concerning the origin of ferromagnetism: no observation of clusters, but the concentration of magnetic ions or carriers is too low to mediate an efficient long range exchange interaction. Indeed, some groups reported they observed magnetic ion-rich nanocrystals by transmission electron microscopy (TEM), but the clusters were embedded artificially.³ There lacks a direct evidence to confirm the existence of magnetic clusters due to the spinodal decomposition in DMSs. In this letter, we report a second ferromagnetic phase transition which is caused by the co-existence of ferromagnetic GeFeTe phase and Fe clusters in $\text{Ge}_{1-x}\text{Fe}_x\text{Te}$ films. It provides direct evidence that the spinodal decomposition exists in DMSs and influences the magnetic property.

$\text{Ge}_{1-x}\text{Fe}_x\text{Te}$ films were deposited on Si (001) substrate by pulsed laser deposition. The structure of the films was analyzed by x-ray diffraction (XRD) and TEM. The magnetic

measurement was performed using a superconducting quantum interference device (SQUID) magnetometer. The transport property was determined by Hall effect measurement.

Figure 1(a) shows the XRD patterns of $\text{Ge}_{1-x}\text{Fe}_x\text{Te}$ films. Only (003), (006), and (009) peaks were observed in the films deposited on Si (001) substrate, indicating a preferred (001) oriented rhombohedral structure.⁵ As the content of Fe increases up to $x=0.38$, some secondary phase of FeTe can be observed. The lattice parameter c of Fe doped GeTe films was found to increase slightly with an increase of Fe content as listed in Table I. Cross-sectional high-resolution TEM (HRTEM) and selected area electron diffraction (SAED) pattern of the films can provide convincing evidence of the

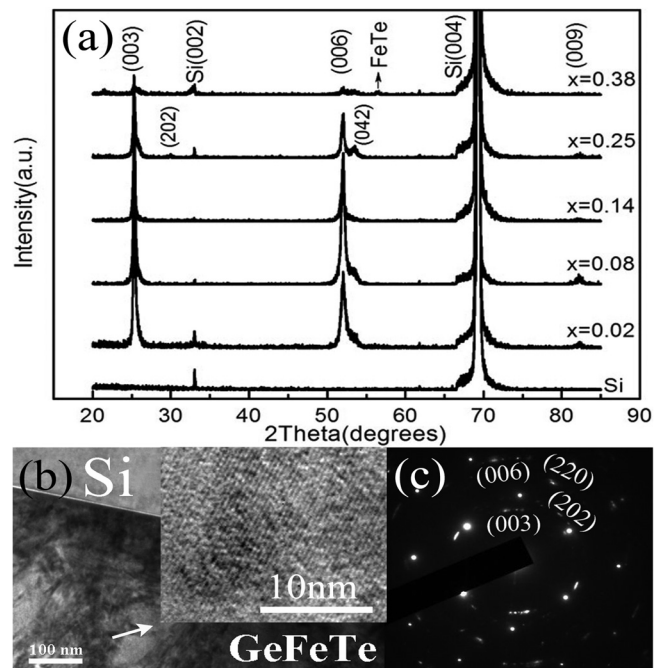


FIG. 1. (a) XRD patterns of $\text{Ge}_{1-x}\text{Fe}_x\text{Te}$ thin films. (b) The cross-sectional TEM of $\text{Ge}_{0.98}\text{Fe}_{0.02}\text{Te}$ film sample, the inset is the HRTEM of the film. (c) The SAED pattern of the cross-section.

^{a)}Authors to whom correspondence should be addressed. Electronic addresses: apjhao@polyu.edu.hk and miaoxs@mail.hust.edu.cn.

TABLE I. Carrier concentration p , resistivity ρ , mobility μ , lattice parameter c at room temperature and saturated magnetization M_s at 2 K of $\text{Ge}_{1-x}\text{Fe}_x\text{Te}$ films.

x	p (10^{20}cm^{-3})	ρ ($10^{-4}\Omega\text{cm}$)	μ (cm^2/Vs)	c (\AA)	M_s (emu/cm^3)
0.02	12.1	3.74	13.8	10.4775	14.9
0.08	3.42	4.55	43.8	10.5414	5.2
0.14	4.51	4.88	29.2	10.5615	4.2
0.25	4.71	3.27	40.9	10.5672	2.0

crystalline across the interface.^{6,7} Figures 1(b) and 1(c) show the cross-sectional HRTEM images and SAED pattern of our film sample, respectively. The images show columnar growth of the film. The SAED pattern confirms that the film is polycrystalline structure corresponding to a rhombohedral lattice. Apparently, no cluster or second phase was observed by both structure measurements when Fe content x is less than 0.25.

Figure 2 shows the magnetic field dependent magnetizations (M - H) of $\text{Ge}_{1-x}\text{Fe}_x\text{Te}$ films with an in-plane magnetic field at 2 K. The saturation magnetizations (M_s) decreased as the content of Fe increased, which could be ascribed to the antiferromagnetic alignment caused by the increased amount of Fe. Similar phenomenon was ever observed in Fe doped In_2O_3 .⁸ The inset shows the M - H curves of $\text{Ge}_{0.98}\text{Fe}_{0.02}\text{Te}$ film under in-plane and out-of-plane magnetic fields. Larger remanent magnetization and coercivity were observed when the magnetic field was applied out-of-plane rather than in-plane, indicating a distinct magnetic anisotropy. Columnar growth of $\text{Ge}_{0.98}\text{Fe}_{0.02}\text{Te}$ film observed by TEM (Fig. 1(b)) as well as the c -axis orientated rhombohedral (ferroelectric phase) structure may lead the magnetic anisotropy.^{9,10}

Figure 3 shows the zero-field cooling (ZFC) and field cooling (FC) temperature dependent magnetization (M - T) curves under different in-plane applied fields for $\text{Ge}_{0.98}\text{Fe}_{0.02}\text{Te}$ film. At low temperatures, a large bifurcation between the ZFC and FC curves and a cusp in ZFC curve are observed, which brings on the central issue in magnetic system: whether the magnetic ground state is a conventional ferromagnet or spin glass or superparamagnetic system.¹¹⁻¹³ It is previously reported that the material with magnetic anisot-

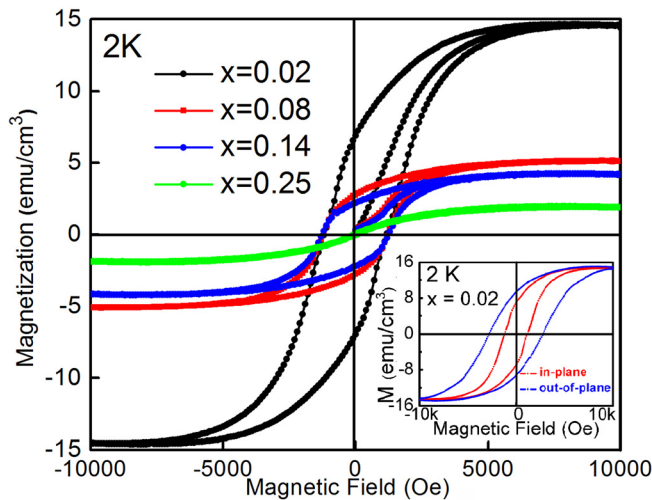


FIG. 2. (Color online) The M - H curves of $\text{Ge}_{1-x}\text{Fe}_x\text{Te}$ films at 2 K. The inset is the M - H curves of $\text{Ge}_{0.98}\text{Fe}_{0.02}\text{Te}$ film under in-plane and out-of-plane magnetic fields.

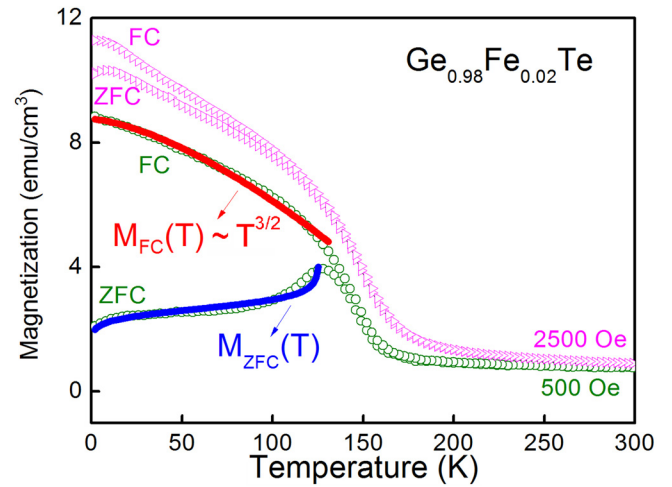


FIG. 3. (Color online) FC and ZFC M - T curves of $\text{Ge}_{0.98}\text{Fe}_{0.02}\text{Te}$ film under applied magnetic field 500 Oe and 2500 Oe. The line is the theoretical simulation by a mean field theory and improved ZFC model.

ropy has an intrinsic long range ferromagnetic property.¹⁴ Next, we will demonstrate that the ferromagnetic behavior is dominated by magnetic anisotropy-related long range ferromagnetic exchange interaction.

It is known that the temperature dependent magnetization of a long range ferromagnetic system can be well depicted by a standard 3D spin wave model which obeys $T^{3/2}$ law.¹⁵ We fitted the FC curve under 500 Oe magnetic field below T_c (Fig. 3). The measured data shows well $T^{3/2}$ dependence, indicating a long range exchange interaction exists in $\text{Ge}_{0.98}\text{Fe}_{0.02}\text{Te}$ film. A modified ZFC model was used to explain the relationship between ZFC measurement and coercive (H_c).¹⁶ In ZFC treatment, the local anisotropic field $\xi(E)$, which can be reflected from $H_c(T)$, resists the alignment of spin to the applied magnetic field. On the other hand, the applied magnetic field (H_A) and the total magnetization (M_{FC}) act to align the spin along the external field. Thus, a simple assumption can be made: M_{ZFC} is proportional to H_A and M_{FC} , but it is inversely proportional to magnetic anisotropy or coercive H_c . We get the following equations:

$$M_{ZFC}(T) \approx kH_A M_{FC}(T)/H_c(T), \quad kH_A \ll H_c, \quad (1)$$

$$M_{ZFC}(T) \approx M_{FC}(T), \quad kH_A \gg H_c, \quad (2)$$

where k is a constant and H_A is a given applied magnetic field. When H_A is large, for example, 2500 Oe, the $M_{ZFC}(T)$ will approximately equal to $M_{FC}(T)$, which can be seen in Figure 3 that the ZFC curve is approximate to the FC curve. In principle, the external magnetic field is large enough to overcome the $\xi(E)$ and rotates the most spin in one direction. While H_A is small, there is a competition among H_A , $\xi(E)$ and thermal magnetic perturbation. We fitted the ZFC curve under the 500 Oe magnetic field. A clear cusp in the simulated curve (temperature above T_c of the M_{ZFC} curve equals to FC, not show in the figure) can be observed, which fits well with the ZFC data (Fig. 3). It gives a complex temperature dependence of $H_c(T)$, not a simple $H_c(T) \propto [M_{FC}(T)]^2$.¹⁶ The reproduction of ZFC measurement by the ZFC model gives further evidence that the ferromagnetism

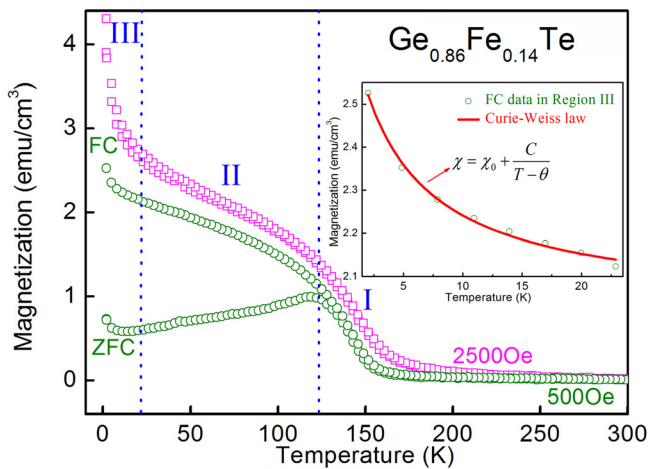


FIG. 4. (Color online) FC and ZFC M - T curves of $\text{Ge}_{0.86}\text{Fe}_{0.14}\text{Te}$ film under applied magnetic field 500 Oe and 2500 Oe. The inset is a simulation by the Curie-Weiss law.

in $\text{Ge}_{0.98}\text{Fe}_{0.02}\text{Te}$ film is dominated by intrinsic ferromagnetic exchange interaction.

Experimentally, we performed transport measurements to establish the relationship between carrier and ferromagnetism in $\text{Ge}_{1-x}\text{Fe}_x\text{Te}$ films shown in Table I. Interestingly, when the maximum value of hole concentration of $1.21 \times 10^{21} \text{ cm}^{-3}$ at $x=0.02$ is reached, both the average magnetic moment for Fe and the whole saturated magnetization get the maximum value, i.e., $4.4 \mu_B$ and 14.9 emu/cm^3 , respectively. While the hole concentrations in higher Fe content films are close with each other and the M_s decreases with increasing Fe content. It shows a dependence of M_s on both hole concentration and Fe content, which is most likely a Ruderman-Kittel-Kasuya-Yosida (RKKY) indirect interaction via carriers. Therefore, it is reasonable to speculate that the observed ferromagnetic phase in $\text{Ge}_{0.98}\text{Fe}_{0.02}\text{Te}$ film is dominated by a long range ferromagnetic exchange interaction via itinerant hole.

Figure 4 shows the FC and ZFC curves of $\text{Ge}_{0.86}\text{Fe}_{0.14}\text{Te}$ film. Regions I and II of the M - T curves indicate a paramagnetic and ferromagnetic phase, which is consistent with $\text{Ge}_{0.98}\text{Fe}_{0.02}\text{Te}$ film. The FC curve and cusp in ZFC curve under the 500 Oe magnetic field can be also depicted by the 3D spin wave and modified ZFC models. It means that region II in Figure 4 is also a ferromagnetic phase caused by RKKY interaction via holes. However, at region III, an abrupt increase of magnetization with decreasing temperature occurs, which differs with the behaviors of $\text{Ge}_{0.98}\text{Fe}_{0.02}\text{Te}$ film. We performed a Curie-Weiss model to fit it.¹⁷ As can be seen in the inset of Fig. 4, the FC curve under 500 Oe at temperature lower than 25 K is reproduced by $\chi = \chi_0 + c/(T - \theta)$, where $c = 2.997 \text{ emuK/cm}^3\text{Oe}$ is the Curie constant and $\theta = -4.067 \text{ K}$ is the Curie-Weiss temperature. The obedience of Curie-Weiss law and the apparent magnetization indicate a superparamagnetic phase for $\text{Ge}_{0.86}\text{Fe}_{0.14}\text{Te}$ thin film at temperature lower than 25 K.¹⁸ It implies the existence of Fe cluster in $\text{Ge}_{1-x}\text{Fe}_x\text{Te}$ system when the Fe content x reaches up to 0.14 which can not be detected by XRD and TEM.

We believe that many of the observed DMSs may contain considerable magnetic clusters mixed with DMS phase,

quite similar to our $\text{Ge}_{0.86}\text{Fe}_{0.14}\text{Te}$ sample. In region II of Fig. 4, the magnetic anisotropy field $\xi(E)$ dominates the magnetization among external magnetic field, thermal magnetic perturbation, and dipole field between Fe clusters. As the temperature decreases to the critical temperature of 25 K, the dipole field increases rapidly due to the decrease of thermal perturbation, resulting in the appearance of a ferromagnetic phase dominated by the superparamagnetic effect.¹⁹ Therefore, we conclude that the ferromagnetic phase transition in $\text{Ge}_{0.86}\text{Fe}_{0.14}\text{Te}$ thin film is from ferromagnet with magnetic anisotropy to superparamagnetic phase at the critical transition temperature of 25 K. There is no second magnetic phase transition in $\text{Ge}_{0.98}\text{Fe}_{0.02}\text{Te}$ film while the doped content increases to $x=0.14$, a distinct ferromagnetic phase transition implying the existence of Fe clusters is observed, which could be considered as a signature of the spinodal decomposition in Fe doped GeTe DMSs.

In summary, we demonstrate that the anomalous ferromagnetic phase transition in $\text{Ge}_{1-x}\text{Fe}_x\text{Te}$ films is due to the co-existence of DMS phase and Fe clusters. Since the clusters in DMSs are hard to detect with conventional crystallographic methods, we consider that the second ferromagnetic phase transition is a direct evidence for spinodal decomposition.

This work was supported by the Hong Kong Polytechnic University Grant (Mainland University Joint Supervision Scheme No. A-SA71) and the National Natural Science Foundation of China (No. 50871043).

- ¹S. A. Wolf, D. D. Awschalom, R. A. Buhrman, J. M. Daughton, S. V. Molnar, M. L. Roukes, A. Y. Chtchelkanova, and D. M. Treger, *Science* **294**, 1488 (2001).
- ²T. Dietl, *Nature Mater.* **5**, 673 (2006).
- ³G. M. Criado, A. Somogyi, S. Ramos, J. Campo, R. Tucoulou, M. Salome, J. Susini, M. Hermann, M. Eickhoff, and M. Stutzmann, *Appl. Phys. Lett.* **86**, 131927 (2005).
- ⁴J. H. Park, M. G. Kim, H. M. Jang, S. R. and Y. M. Kim, *Appl. Phys. Lett.* **84**, 1338 (2004).
- ⁵JCPDS-ICCD Powder Diffraction Pattern File (PDF-2) Card No. 47-1079.
- ⁶J. S. Wu, C. L. Jia, K. Urban, J. H. Hao, and X. X. Xi, *J. Mater. Res.* **16**, 3443 (2001).
- ⁷J. H. Hao, J. Gao, Z. Wang, and D. P. Yu, *Appl. Phys. Lett.* **87**, 131908 (2005).
- ⁸X. H. Xu, F. X. Jiang, J. Zhang, X. C. Fan, H. S. Wu, and G. A. Gehring, *Appl. Phys. Lett.* **94**, 212510 (2009).
- ⁹P. Sharma, H. Kimura, and A. Inoue, *Phys. Rev. B* **78**, 134414 (2008).
- ¹⁰M. Venkatesan, C. B. Fitzgerald, J. G. Lunney, and J. M. D. Coey, *Phys. Rev. Lett.* **93**, 177206 (2004).
- ¹¹W. Q. Chen, K. L. Teo, S. T. Lim, M. B. A. Jalil, T. Liew, and T. C. Chong, *Appl. Phys. Lett.* **90**, 142514 (2007).
- ¹²T. E. Quicke, V. H. Le, T. Brezesinski, and S. H. Tolbert, *Nano Lett.* **10**, 2982 (2010).
- ¹³A. Malinowski, V. L. Bezusyy, R. Minikayev, P. Dziawa, Y. Syryanyy, and M. Sawicki, *Phys. Rev. B* **84**, 024409 (2011).
- ¹⁴P. Sati, R. Hayn, R. Kuzian, S. Regnier, S. Schafer, A. Stepanov, C. Morhain, C. Deparis, M. Laugt, M. Goiran, and Z. Golacki, *Phys. Rev. Lett.* **96**, 017203 (2006).
- ¹⁵S. J. Potashnik, K. C. Ku, R. Mahendiran, S. H. Chun, R. F. Wang, N. Samarth, and P. Schiffer, *Phys. Rev. B* **66**, 012408 (2002).
- ¹⁶D. L. Hou, E. Y. Jiang, G. D. Tang, Z. Q. Li, S. W. Ren, and H. L. Bai, *Phys. Lett. A* **298**, 207 (2002).
- ¹⁷J. C. A. Huang, H. S. Hsu, Y. M. Hu, C. H. Lee, Y. H. Huang, and M. Z. Lin, *Appl. Phys. Lett.* **85**, 3815 (2004).
- ¹⁸C. P. Bean and J. D. Livingston, *J. Appl. Phys.* **30**, 120S (1959).
- ¹⁹T. Jonsson, P. Nordblad, and P. Svedlindh, *Phys. Rev. B* **57**, 497 (1998).